

Interfacial energy induced microstructure of thin magnetic iron/gold multilayer films

C. BORCHERS, P. TROCHE, C. HERWEG, J. HOFFMANN
*Institute of Materials Physics, University of Göttingen, Hospitalstr. 3-7,
 37073 Göttingen, Germany*
E-mail: chris@umpa03.gwdg.de

Magnetron sputtered iron/gold multilayers are investigated by cross-sectional transmission electron microscopy. Thermodynamic considerations can explain the different observed microstructures near the substrate and near the top of the multilayers. © 2002 Kluwer Academic Publishers

1. Introduction

Thin film multilayer structures are of great interest in current research. Different multilayer systems are used for example for lasers [1], magnetic memories (MRAM), X-ray mirrors [2], or magnetic sensors (Giant Magnetic Resistance) depending on the scaling and the materials the single layers are made of. However, to reach reproducible abilities of the applications, the multilayer parameters, i.e. the layer thicknesses and interface roughness and flatness, must be controlled carefully. Therefore, the physical reasons for any observed multilayer morphology has to be understood profoundly. Furthermore, the long time thermal stability of multilayers is a precondition for any kind of practical application [3, 4]. The dependance of the thermal stability of Fe/Au multilayers on the interface roughness was investigated by Troche and coworkers [5]. They found that the driving forces of a disintegration of the layered structure was the stronger, the stronger the curvature of the interfaces was. It is the aim of this work to establish the microstructure of as-prepared magnetron sputtered Fe/Au multilayers and to discuss the observed results in terms of thermodynamics, especially in view of possible interface curvatures.

2. Experimental

Fe/Au multilayers were prepared by magnetron sputtering. They consist of 70 bilayers of Fe 2 nm/Au 10 nm on Si (110) substrate. The samples were prepared for cross-sectional electron microscopy in the usual manner. Electron microscopy was performed on a Philips EM 420 ST. Magnetic measurements were performed with an Oxford low-temperature vibrating sample magnetometer (VSM) with superconducting magnets. The maximum applicable field is 5 T, minimal stepsize is 0.001 T/min. Measurements were performed at room temperature.

3. Results

Fig. 1a shows an overall view of a Fe/Ag multilayer with 70 layer pairs Fe 2 nm/Au 10 nm. The substrate is marked. The Au layers appear dark, and the Fe layers

appear bright. Near the substrate, the Fe layers are fairly straight, and the Au layers show heavy strain contrast in form of oscillating brightness within the individual layers. Near the top of the multilayer, the layers are arched towards the top of the multilayer with a period of ~ 30 nm, a height of ~ 10 nm, and the contrast within the layers is quite uniform. In spite of the observed arching, the thickness of the individual layers does not vary much. Fig. 1b shows a dark field micrograph of the same region. The bright grain indicated by an arrow reveals a lateral Au grain size on the order of the layer thickness. The bright regions extending over up to ~ 20 bilayers and a lateral extension of about 50 to 100 nm have the same orientation. This shows that the multilayer structure is strongly texturized, and a given Au grain can communicate its orientation throughout the Fe layer to the Au in the adjacent layer. The diffraction image Fig. 2 shows a ring pattern that can be identified as a fcc pattern. In Fig. 3, high resolution images of the multilayer can be seen. Fig. 3a shows a region near the substrate, 3b shows a region in the middle of the stack. The Au (111) lattice fringes are resolved. They are parallel to the substrate interface, even at places where the interface between neighbouring Au and Fe layers is not. The Fe lattice fringes could not be resolved. The interface roughness is up to 1 nm. In 3b, a severely disturbed region is imaged. Even here, the (111) lattice fringes retain their parallelity. Fig. 3c shows another set of (111) lattice fringes. Here, the fringes seem to pass through the Fe layers, but at the places where the Fe layers are, the fringes show some disturbances resembling microtwins. There is a twin boundary in the Au layer with the boundary normal parallel to the growth direction at the place marked with an arrow. Several thus arranged twin boundaries could be found in the multilayers.

In Fig. 4, magnetic measurements of a (Fe 2 nm/Au 10 nm) \times 150 multilayer is shown. A saturation magnetization of 0.0160 emu was observed. Referring to the sample geometry, i.e. the sample area of (7 \times 5.5) mm² and the added up Fe-layer thicknesses of 300 nm, this corresponds to an average magnetic moment of 1.9 μ .

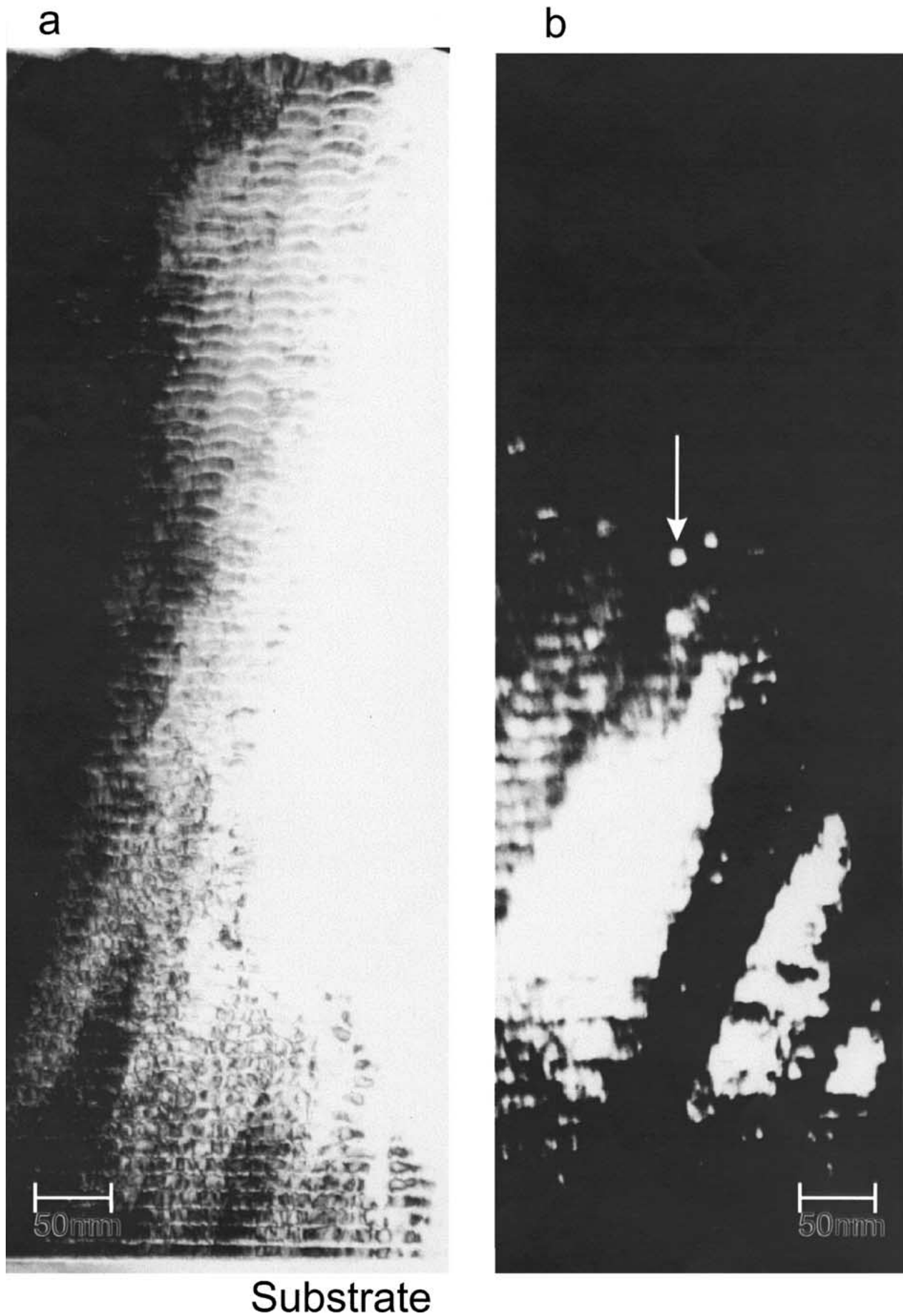


Figure 1 (a) Overall view of a $(\text{Fe } 2 \text{ nm}/\text{Au } 10 \text{ nm}) \times 70$ multilayer. Au layers appear bright, Fe layers appear dark. (b) Dark field of the same region.

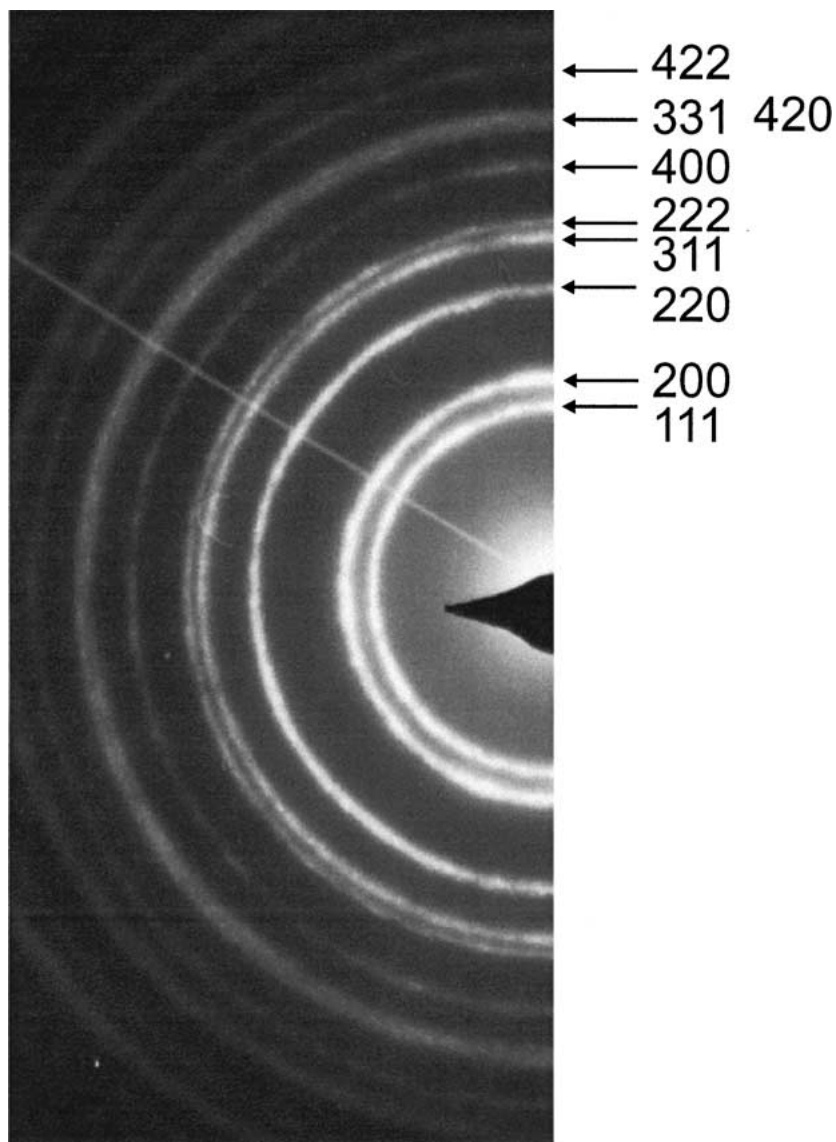


Figure 2 Corresponding diffraction image. Rings are marked for fcc.

4. Discussion

The structure of the iron layers is not evident, since the diffraction images exhibit a ring structure characteristic for a fcc lattice. In Table I, the relative width of the expected rings for fcc Au: $a = 4.07 \text{ \AA}$, and bcc Fe: $a = 2.87 \text{ \AA}$ as well as fcc Fe: $a = 3.65 \text{ \AA}$. Au{111} is

TABLE I Relative width of diffraction rings for fcc Au: $a = 4.07 \text{ \AA}$, bcc Fe: $a = 2.87 \text{ \AA}$, and fcc Fe: $a = 3.65 \text{ \AA}$. Au{111} is set as width 1

fcc Au	Width	bcc Fe	Width	fcc Fe	Width
111	1.00			111	1.12
200	1.15	110	1.16	200	1.29
220	1.63	200	1.64	220	1.82
311	1.92			311	2.14
222	2.00	211	2.01	222	2.23
400	2.31	220	2.32	400	2.58
331	2.52			331	2.81
420	2.58	310	2.60	420	2.88
422	2.83	222	2.84	422	3.15
333	3.00	321	3.06	333	3.35
440	3.27			440	3.65
531	3.42			531	3.83
442	3.46	330	3.47	442	3.87

set as width 1. It is clear that if iron was fcc, it could be seen in the diffraction patterns. The rings for bcc iron fall on gold rings with an accuracy that does not allow to differentiate between them in the diffraction images. So if Fe is crystalline in these multilayers, it is bcc. From the point of view of electron diffraction, Fe might be amorphous for small layer thicknesses like 2 nm. With a Fe 2 nm/Au 10 nm stacking, the amorphous halo would be too weak to be distinguished from background scattering. However, it is known that the ground state magnetization of amorphous iron decreases to 1.2μ and the Curie temperature is lowered significantly with respect to bcc iron [6, 7]. The measured magnetic moment is 1.9μ , a value which is near the bulk value of bcc iron (2.2μ). The difference between the magnetic moment of bulk iron and iron in these multilayers can be explained by perturbed interfaces in the multilayer. The observations suggest that the structure of the Fe layers is bcc. Furthermore, for a 2.5 nm amorphous Fe film, that was deposited at 4 K [8], a crystallization transition at 50 K with a width of less than 5 K was found. This too confirms that Fe should be in a crystalline state in our films. The main observation in the survey of the

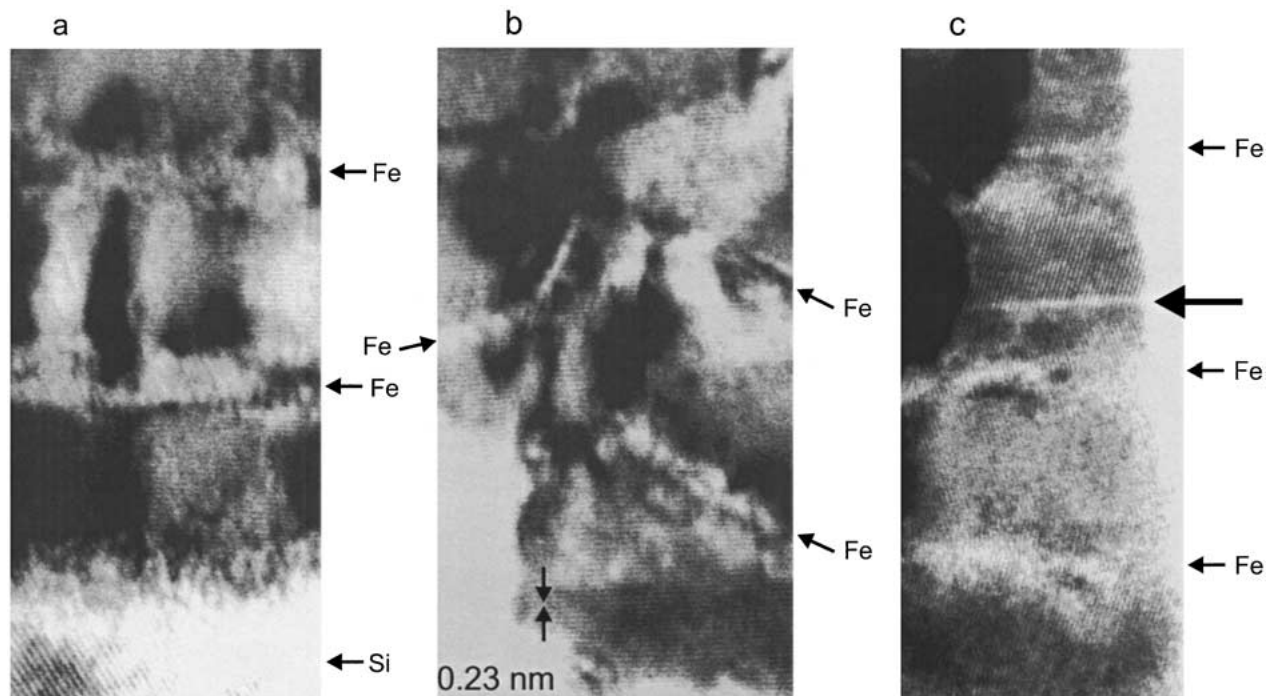


Figure 3 (a) High resolution image of a region near the substrate. For details, see text. (b) High resolution image of a severely disturbed region. For details, see text. (c) High resolution image with twin boundaries. For details, see text.

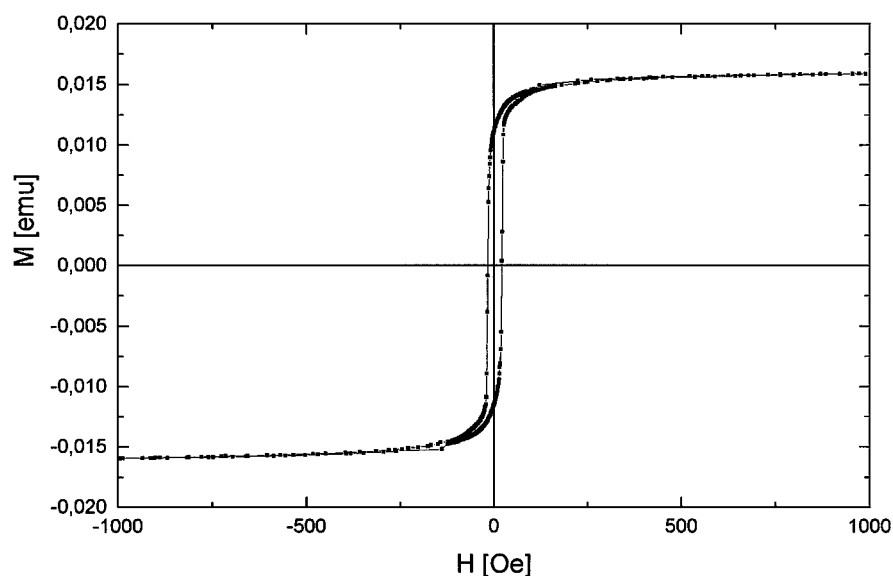


Figure 4 Hysteresis loop at $T = 292$ K for a multilayer of $150 \times (1.8 \text{ nm Fe}/10 \text{ nm Au})$ coercivity $H(c) = 20$ Oe, saturation magnetization $M(S) = 0,016$ emu.

(Fe 2 nm/Au 10 nm) \times 70 multilayer, see Fig. 1, is that the layers near the substrate are smooth, and that there seem to be high stresses in the Au layers. Near the top of the stack, the interfaces are arched, but the strain contrast is much less pronounced than on the substrate side, so the stress seems to be smaller there. Tersoff and LeGoues [9] state that for high misfits over 1%, surface roughening is the primary mechanism to relax misfit strains. Jesson [10] describes that such roughnesses tend to develop a characteristic length scale, as can be seen in Fig. 1a of this work.

In our case, body centered cubic iron can be expected to grow in local Nishiyama-Wassermann orientation relationship [11, 12] on gold, as is reported for Fe/Ag

multilayers [13]. This is supported by the HRTEM micrograph in Fig. 3a, where Au $\langle 111 \rangle$ fringes can be seen to be normal to the growth direction. The dark field micrograph Fig. 1b shows that subsequent gold layers tend to have the same in-plane orientation, which also supports the assumption of a local epitaxial growth of Fe on Au and vice versa. There is an in-plane texture on a scale of 50 to 100 nm, and an out-of-plane texture over the whole stack. This was also reported by Herweg [14].

It is remarkable that the Au layers do not give up their $\langle 111 \rangle$ texture, even though it goes along with a considerable strain energy when the interface is parallel to the substrate, or, on the other hand, the area of the interface is enlarged compared to a flat interface,

when it is arched. When deposited onto a Si substrate, there is an amorphous native oxide with a thickness of about two to three nanometers. On this oxide, the Au forms close packed layers. Obviously the orientation, out-of-plane as well as in-plane, of the Au is resumed in subsequent Au layers through the two nanometer of Fe, no matter whether the interface is flat or not, as it was also described by Jesson [10]. It seems most probable that the arched interfaces are arranged in steps parallel to $\langle 111 \rangle$ Au or $\langle 110 \rangle$ Fe, respectively, so that the orientation relationship can be maintained, but the high stresses in one direction can be absorbed by the steps, leading to an interfacial energy comparable to that of a high angle grain boundary plus chemical contribution, without giving up the orientation relationship. This allows for a relaxed arrangement with respect to strain, but does not force the system to give up coherency. These considerations are in agreement with the high resolution image Fig. 3b, where the lattice fringes can be seen to go through the iron layers. In Fig. 3c, twinning parallel to the substrate can be seen, as well as some microtwinning near the iron layer. Twinning is also known to occur when stress has to be relieved.

For an epitactical Au thin film grown on Fe in Nishiyama-Wassermann orientation relationship, the coherency stress can be estimated as follows: The misfit is strongly anisotropic. In the $\langle 100 \rangle_{bcc}$ direction, which is parallel to $\langle 110 \rangle_{fcc}$, the misfit ϵ_x is 0.0035. In the $\langle 011 \rangle_{bcc}$ direction, which is parallel to $\langle 11\bar{2} \rangle_{fcc}$, the misfit ϵ_y is 0.185. The homogeneous strain energy density e_{hom} is given by

$$e_{hom} = 2\mu \frac{1+\nu}{1-\nu} \epsilon^2 \quad (1)$$

where μ is the shear modulus, ν the Poisson ratio. The shear modulus of Fe $\mu_{Fe} = 11.07 \times 10^{10}$ J/m³ [15] is almost three times as large as the shear modulus of gold, $\mu_{Au} = 4.23 \times 10^{10}$ J/m³ [15]. The strain energy can therefore be expected to be accommodated mainly in the gold layers. For a Au film with a layer thickness $t = 10$ nm on a semi-infinite Fe substrate, the homogeneous strain energy density in $\langle 110 \rangle_{fcc}$ direction amounts to $\sim 2 \times 10^6$ J/m³. In $\langle 11\bar{2} \rangle_{fcc}$ direction without misfit dislocations, it amounts to $\sim 5.8 \times 10^9$ J/m³ for an epitactical semi-infinite interface. The strain energy might be lessened by the introduction of misfit dislocations, but it is known that this is difficult in nano-sized particles or grains [16]. So this enormous misfit strain energy has to be taken up by the gold grains in case of epitactical growth and flat interfaces. In agreement with this, in Fig. 1 a pronounced strain contrast can be seen in the gold layers near the substrate, where the layer interfaces are flat. Near the surface of the multilayer, the iron layers are arched, and the strain contrast in the gold layers has lessened noticeably. It was ascertained that this arching does not go along with a bending of the lattice planes. Therefore, this arching destroys the long-scale epitaxy without destroying the orientation relationship and so helps reduce the strain energy. Instead, the energy of an incoherent boundary has to be raised. The energy balance of this process can

be estimated as follows: The chemical contribution to a coherent as well as an incoherent Fe/Au boundary can be taken to be negligibly small or even positive, since the interaction between Fe and Au is attractive [17], and the chemical contribution to interfacial energies can be estimated by the pair interaction energy between the two species sharing the interface [18]. The structural contribution to the interfacial energy of an incoherent Fe/Au boundary can be expected to be on the order of $\gamma_{incoh} \approx 1$ J/m², which is about the energy of an incoherent grain boundary. The structural contribution to the interfacial energy of an epitactical Fe/Au interface in Nishiyama-Wassermann relationship without misfit dislocations can be estimated as $\gamma_{coh} = e_{hom}t/2$, where t is the layer thickness. The homogeneous strain energy corresponds to an interfacial energy of ~ 30 J/m², which is extremely high. So if the coherency is given up, much of the interfacial energy can be spared, even when the area of the interface is enlarged. Since the Au layers are less stressed in the regions where the layers are arched, above considerations seem to be reasonable.

5. Conclusions

In this work it was shown that sputtered Fe 2 nm/Au 10 nm multilayers exhibit bcc iron growth with Nishiyama-Wassermann orientation relationship between the Fe and Au layers. Near the Si substrate, the interfaces are flat and the Au layers are heavily strained. Near the top of the multilayer, the interfaces are arched with a period of ~ 30 nm and an arch height of ~ 10 nm. Here the strain in the layers has decreased to a high extent. There is strong texture, as well in-plane as out-of-plane. Regions with a lateral extension of ~ 30 – 100 nm are texturized through the whole layer stack. This necessitates local epitaxial growth between the Fe and Au layers over similar areas, which causes high strain energies in one direction for Nishiyama-Wassermann growth. These strain energies can be released by the arching of the interfaces without destroying the orientation relationship.

References

1. M. WUTTIG, "Physik der Nanostrukturen" (Jülich, 1998).
2. C. MICHAELSEN, P. RICARDO, D. ANDERS, M. SCHUSTER, J. SCHILLING and H. GÖBEL, *Adv. X-Ray Anal.* **42** (2000) 308.
3. P. TROCHE, J. HOFFMANN, K. HEINEMANN, F. HARTUNG, G. SCHMITZ, H. C. FREYHARDT, D. RUDOLPH, J. THIEME and P. GUTTMANN, *Thin Solid Films* **353** (1999) 33.
4. D. J. BEKE, G. LANGER, M. KIS-VARGA, A. DUDAS, P. NEMES, L. DAROCZI, G. KERÉKES and Z. ERDELYI, *Vacuum* **50** (1998) 373.
5. P. TROCHE, *MRS Proceedings* 1999, to be published.
6. K. PRÜGL, Ph.D. thesis, Regensburg, 1999.
7. Y. KAKEHASHI and T. UCHIDA, *Phys. Rev. B* **56** (1997) 8807.
8. P. K. LEUNG and J. G. WRIGHT, *Phil. Mag.* **30** (1974) 995.
9. J. TERSOFF and F. K. LEGOUES, *Phys. Rev. Lett.* **72** (1994) 3570.
10. D. E. JESSON, in "Handbook of Thin Film Process Technology," edited by D. A. Glocker and S. J. Shah (IOP Publishing, Bristol, 1977) p. F1:6.
11. Z. NISHIYAMA, *Scient. Rep. Tohoku Univ.* **23** (1934) 638.
12. G. WASSERMANN, *Arch. Eisenhüttenw.* **16** (1933) 647.

13. S. I. POPEL, V. N. KOZHURKOV and A. A. ZHUKOV, *Russian Metal* **5** (1975) 56.
14. C. HERWEG, Diploma Thesis, Göttingen, 1999.
15. R. F. S. HEARMON, in "Landolt-Börnstein New Series III" Vol. 11, edited by K.-H. Hellwege and A. M. Hellwege (Springer, Heidelberg, 1979) p. 9.
16. J. WEISSMÜLLER, private communication.
17. L. SWARTZENDRUBER, *Bull. Alloy Phase Diag.* **5** (1984) 592.
18. R. BECKER, *Ann. Phys.* **32** (1938) 128.

*Received 14 March
and accepted 4 October 2001*